ELSEVIER

Journal of Molecular Catalysis A: Chemical 179 (2002) 213–220

JOURNAL OF MOLECULAR CATALYSIS A: CHEMICAL

www.elsevier.com/locate/molcata

Phase transformations in the thermoactivated MnO_x–Al_2O_3 catalytic system

P.G. Tsyrulnikov [a], S.V. Tsybulya [b,*], G.N. Kryukova [b], A.I. Boronin [b], S.V. Koscheev [b], T.G. Starostina [b], A.V. Bubnov [a], E.N. Kudrya [a]

[a] *Omsk Branch of Boreskov Institute of Catalysis, Neftezavodskaya Str. 54, Omsk 644040, Russia*
[b] *Boreskov Institute of Catalysis, pr. Lavrentieva 5, Novosibirsk 630090, Russia*

Received 19 April 2001; accepted 17 August 2001

Abstract

The phenomenon of the sharp increase of activity in reactions of deep oxidation found for the manganese oxide–alumina system calcined at 900–1000 °C was named as thermoactivation effect. This effect was shown to be associated with phase transformations in this system. Peculiarities of phase transformations in the MnO_x/Al_2O_3 system after its calcination at 950 °C for 1–10 h were studied with XRD, TEM, XPS methods; the catalysts activity in deep oxidation of *n*-pentane was measured in a flow-circuit setup. It was found that a set of phase transformations occurred in the system, starting from the formation of the metastable nonstoichiometric manganese–alumina cubic spinel (after 1–2 h calcination) and nonequilibrium solid solution of Mn^{3+} ions in the structure of γ-Al_2O_3 which decomposes producing high-temperature aluminas modified by manganese ions and particles of imperfect β-Mn_3O_4 phase doped with aluminium ions. Increase of the calcination time to 10 h and more results in the formation of biphasic system composed of α-Al_2O_3 and nanocrystalline β-Mn_3O_4 modified by Al^{3+} ions. These transformations are associated with the maximum activity showed by catalysts calcined for 5–6 h in the reaction of *n*-pentane combustion.

Keywords: MnO_x/Al_2O_3 catalyst; Calcination; Phase transformation; XRD; TEM; XPS

1. Introduction

It has been shown [1,2] that when lean gas mixtures are burnt by using the reverse-process technology, one may accumulate heat in the reactor up to rather high temperatures and utilize it. In this case, temperature-resistant catalysts are strongly needed. Therefore, we began to develop a combustion catalyst with a high resistance to temperatures up to 1000 °C. At present this catalyst is registered as IC-12-40 (known in USA as Z-2 [3]) and commercially produced by "Katalizator" in Novosibirsk, Russia.

Numerous studies devoted to the temperature-resistant combustion catalysts are available. The data obtained are surveyed in reviews [4–6]. The main purpose of these reviews was to analyse the possibility of producing the catalysts with good resistance to super high temperatures and applying them for methane combustion in various devices, in particular, in gas turbines operating at temperatures up to 1400 °C. As shown in [4], the main objects under research among the oxide systems were the derivatives of manganese hexa-aluminates, which contain alkali and rare-earth ions. IC-12-40

* Corresponding author.
E-mail address: tsybulya@catalysis.nsk.su (S.V. Tsybulya).

1381-1169/02/$ – see front matter
PII: S1381-1169(01)00327-2

1. $(500^0 - 800^0) \rightarrow \gamma\text{-}Al_2O_3 + \beta\text{–}MnO_2 \rightarrow [\gamma\text{-}Al_2O_3 - Mn^{+3}] + \alpha\text{-}Mn_2O_3 \longrightarrow$

2. $(900^0) \rightarrow \mathbf{[\beta\text{-}Mn_3O_{4+x}\text{–}\ Al^{+3}]}\ + [\delta\text{ - }Al_2O_3\text{ - }Mn^{+3}] + [\alpha\text{ - }Al_2O_3\text{ - }Mn^{+3}] \rightarrow$

3. $(1000^0) \rightarrow \mathbf{[\beta\text{-}Mn_3O_4\text{–}\ Al^{+3}]} + [\delta\text{-}Al_2O_3\text{ - }Mn^{+3}]_{traces} + [\alpha\text{ - }Al_2O_3\text{ - }Mn^{+3}] \rightarrow$

4. $(1100^0) \longrightarrow Mn_{1+x}Al_{2-x}O_4 + [\alpha\text{ - }Al_2O_3\text{ - }Mn^{+3}]$

Scheme 1.

catalyst, being a simpler binary MnO_x–Al_2O_3 system, is intended for operation at temperatures up to 1000 °C.

Thermal activation effect is very characteristic for the IC-12-40 catalyst. It has been found previously [7] that calcination of $MnO_x/\gamma\text{-}Al_2O_3$ in air at the temperature range 900–1000 °C causes a sharp increase (10-fold and more) of the activity of this catalyst in the reaction of deep oxidation of hydrocarbons. This phenomenon has been referred to as "thermal activation effect". XPS data [7,8] showed that this effect is manifested as an increase in the Mn/Al ratio on the catalyst surface that might indicate on the process of dispersion of the supported manganese oxide in this temperature interval.

Studies of supported manganese–alumina catalysts calcined at different temperatures [7–10] have shown that at 500–800 °C solid solutions of Mn^{3+} in the alumina structure are formed due to the partial dissolution of manganese ions. But the main part of manganese is still in the form of $\alpha\text{-}Mn_2O_3$ oxide phase. Calcination of the system at higher temperatures (900–1000 °C) results in the decomposition of these solutions and formation of corundum and manganese oxide nanoparticles. According to XRD and EXAFS, the latter structure can be identified as an imperfect spinel of the $\beta\text{-}Mn_3O_4$ type. The imperfection, characterized by the Mn–Mn distances which differ from those in the ideal spinel is associated with modification of the structure of manganese oxide nanoparticles by Al^{3+}ions. Formation of thermodynamically more stable phases (corundum and spinel) is the driving force for the phase transformation processes in the system. The presence of manganese atoms in the alumina structure facilitates the transformation of $\gamma\text{-}Al_2O_3$ into corundum as registered by XRD already in the sample calcined at 900 °C (70% of α-alumina after 900 °C and 6 h [7]).

Phase transformations that occur in the systems as a function of calcination temperature (after 6 h calcination time) are presented in Scheme 1 according to data of EXAFS, XRD, TEM and chemical analysis [8–10], where square brackets are used for designation of the solid solutions of the definite structures. As evident from this scheme, firstly the transformation of $\beta\text{-}MnO_2$ into $\alpha\text{-}Mn_2O_3$ is only observed in the temperature region of 500–800 °C (stage 1). At this stage, some Mn^{3+} ions may be dissolved within the structure of $\gamma\text{-}Al_2O_3$ [9]; however, this does not cause the noticeable change of the alumina crystal lattice parameters. At calcination temperatures of 900–1000 °C (stages 2 and 3) transformations of $\alpha\text{-}Mn_2O_3$ and $\gamma\text{-}Al_2O_3$ into $\beta\text{-}Mn_3O_4$ and $\delta\text{-}Al_2O_3$ ($\alpha\text{-}Al_2O_3$) take place, respectively. As a result, solid solutions based on the structures of tetragonal spinel of $\beta\text{-}Mn_3O_4$ and $\delta\text{-}Al_2O_3$ are formed. Raising the temperature over 1000 °C (stage 4) leads to the formation of crystalline phases of $\alpha\text{-}Al_2O_3$ and cubic aluminium–manganese spinel of variable composition.

Note that by washing off the active component from the corundum surface with acidified KI solution, we succeeded to determine the composition of the active clusters by means of chemical analysis. The compositional data agree well with the data of differential phase dissolving analysis [10].

The aim of this work was to study the peculiarities of phase transitions in the MnO_x–Al_2O_3 catalytic system using XRD, TEM and XPS.

2. Experimental

The support, $\gamma\text{-}Al_2O_3$ ($S = 156\,m^2/g$, total pore volume $\sim 0.45\,cm^3/g$), was purchased from Siberian Catalyst. It was impregnated to incipient wetness with a solution of $Mn(NO_3)_2{\cdot}6H_2O$ (chemical purity

grade) to adjust the content of the active component, β-MnO_2, in the final catalyst to 10 wt.%. The samples were kept at ambient temperature for 12–14 h, then dried in an oven at 120 °C for 6 h. Then the first series of samples were placed in a furnace at room temperature and heated to 950 °C for 1 h and kept at this temperature for a present time period (1–10 h). The dried catalysts of the second series were calcined at 700 °C for 4 h, and then put into a furnace heated to 950 °C and kept at this temperature from 1 to 6 h (time interval between the samples was 1 h).

The activity of each catalyst was measured in a flow-circuit setup for the model reaction of *n*-pentane combustion at 300 °C. The inlet and outlet concentration of *n*-pentane were 0.1 and 0.05 vol.%, respectively.

XRD analysis was performed on a DRON-3 (Russia) and URD-6 (Germany) X-ray diffractometers on Cu Kα or Co Kα radiation and graphite monochromator. XPS characterization of the samples was done with a VG ESCALAB (VG Scientific, GB) electron spectrometer. Emission of electrons from the samples was achieved by soft X-ray irradiation (Mg Kα), so that the mean free path, λ, equalled 20–30 Å depending on the analysed line. Hence, the available depth of the subsurface catalyst layer was ∼3λ or 60–90 Å. The element ratios were determined from integer intensities of corresponding peaks with account of the atomic sensitivity factors. The substraction of background was performed by using Shierly's procedure [11].

TEM studies were performed with a JEM-2010 (Japan) microscope operating at 200 kV accelerating potential. Samples for TEM work were prepared from ethanol slurry followed by deposition of a drop of suspension onto the holey carbon films.

The surface area was measured by the BET method using nitrogen adsorption at 77 K and $(p/p_0)_{eq} = 0.178$ in a "Sorpty-1750" setup.

3. Results and discussion

3.1. XRD and TEM studies

XRD analysis indicates that after a 4 h calcination at 700 °C the catalyst consists of biphasic system, MnO_x–Al_2O_3 [7]. However, as shown recently [9], at this temperature some of the manganese atoms (Mn^{3+}) are dissolved in the structure of γ-Al_2O_3 thus producing a solid solution. According to the XRD pattern of the sample calcined at 950 °C for 4 h (Fig. 1), the system consists of α-Al_2O_3 + δ-Al_2O_3 + β-Mn_3O_4* phases. A similar sample calcined for 3 h has the same phase composition. As shown in [10], the phase Mn_3O_4* is a solid solution of Al^{3+} ions (10–15 at.%) within the micrograined structure of Mn_3O_4.

The absolutely new observation is the appearance of XRD peaks corresponding to well-crystallized phase of $Mn_{2-x}Al_{1+x}O_4$ cubic spinel in the XRD patterns of the samples calcined for 1–2 h at 950 °C (see Fig. 1), although earlier studies [9,10] showed that cubic spinel is formed only at temperatures above 1000 °C and remains stable under extended heating. Nevertheless, in the present case the increase of calcination time lead to disappearance of the imperfect metastable cubic spinel phase. It is known from literature [12,13] that well-crystallized phases of nonstoichiometric binary oxides with "protospinel" structure could be formed on the basis of γ-Al_2O_3 at a limited temperature range. Indeed, in magnesium–alumina system such nonstoichiometric phases had proven to be stable till 1000 °C and to decompose to stoichiometric spinels and α-Al_2O_3 at elevated temperature [13]. The presence of particular extended defects in the structure of these materials [14] seems to be a reason for their relative stability. Annealing of the defects leads to the structural decomposition of "protospinels". It seems likely that in our system the nonstoichiometric defect spinels are formed as intermediate protospinels. Owing to their metastability, the formation of the α-Al_2O_3 phase can start at a relatively low temperatures.

According to the JCPDS data [15], the manganese–alumina phase found in the 10%MnO_x/Al_2O_3 sample calcined at 950 °C for 1 h was identified as Mn_2AlO_4; after a 2 h calcination, the phase composition remained almost the same—$Mn_{1.8}Al_{1.2}O_4$. As the sample was calcinated for 3 h, reflections of this phase disappeared, at the same time the broad peaks of β-Mn_3O_4 imperfect tetragonal phase arised and remained practically unchanged after a 4 h calcination of the sample (Fig. 1). The support consisted predominantly of α-Al_2O_3 and small amount of δ- and θ-Al_2O_3 modified by Mn^{3+} ions.

In the XRD patterns of the samples calcined for 5 h and longer, the support is of α-Al_2O_3 whereas

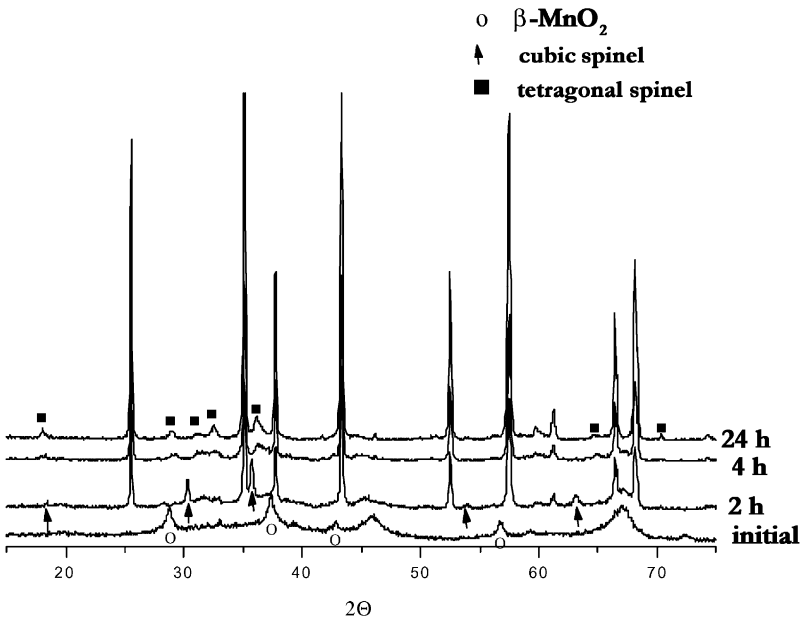

Fig. 1. XRD patterns of the catalyst calcined at 950 °C for different time intervals.

the active component is represented by broad, low-intensity reflections of manganese oxide. As shown earlier [9,10], these reflections correspond to an imperfect Al^{3+}-doped β-Mn_3O_4 spinel with a particle size of about 60 Å. The samples calcined at 950 °C for 8 and 10 h are characterized by a gradual disappearance of the modified δ-Al_2O_3 phase; the phase of manganese oxide is dispersed; and the support is represented by corundum.

Extended (10 h and longer) calcination of the catalysts at 950 °C in air indicates that particles of β-Mn_3O_4 show the same particle size (∼60 Å) as those in the samples calcined for 5 h. Surprisingly, the particle size of the active phase does not change even after the 800 h calcination of sample at 950 °C in air [16]. It seems reasonable to suppose that prolonged calcination facilitates the transformation of the imperfect spinel particles modified by Al^{3+} ions yielding small micrograined crystals of β-Mn_3O_4 doped with Al atoms. It is likely that the latters are located predominantly in the vicinities of the micrograin boundaries in β-Mn_3O_4 particles and act as a structural sintering preventing barrier against annealing of the oxide nanocrystals.

XRD studies of samples calcined at 950 °C for 1 and 2 h revealed the presence of a cubic manganese–alumina spinel with a composition close to Mn_2AlO_4 spinel but the observed phase is proven to be unstable. Therefore, it was suggested that this observed phase might have a particular microstructure. TEM data obtained for this samples showed that along with γ-Al_2O_3 particles and small amount of the manganese oxide they contained spinel microcrystals having a particular microstructure. Its most important peculiarity is the presence of specific defects which appear as a result of vacancy coalescence in the nonstoichiometric spinel during its formation. Typical micrograph of this structure is shown in Fig. 2, where defects in the form of pseudohexagonal closed loops are arrowed. Similar defects were observed earlier [13] in the structure of the nonstoichiometric magnesium–alumina spinel, but in a much lower concentration, and in γ-Al_2O_3 produced by thermal decomposition of well-crystallized boehmite [14]. The mechanism of the formation of such particular defects in the nonstoichiometric spinels is assumed to be the ordering of cation vacancies on the dislocation walls. It seems reasonable to expect that the observed manganese–alumina cubic spinel which is

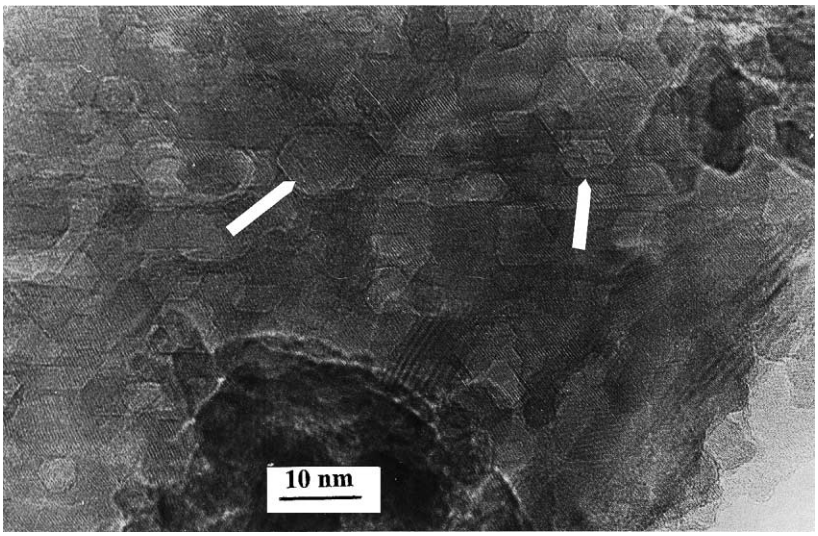

Fig. 2. Micrograph of 10%MnO_x–Al_2O_3 calcined 1 h at 950 °C. Characteristic pseudohexagonal loops are marked by arrows.

formed as a result of the chemical transformation of α-Mn_2O_3 and diffusion of Al^{3+} possesses a lack of bivalent (Mn^{2+}) cations and, hence, high concentration of the cation vacancies. As evident from the micrograph of 10%MnO_x/Al_2O_3 calcinated for 3 h at 950 °C (Fig. 3), this temperature regime initiates the transformation of the nonstoichiometric spinel to α-Al_2O_3 and nanocrystalline β-Mn_3O_4*. These conclusions derived from TEM micrographs are in a good accordance with those derived from XRD.

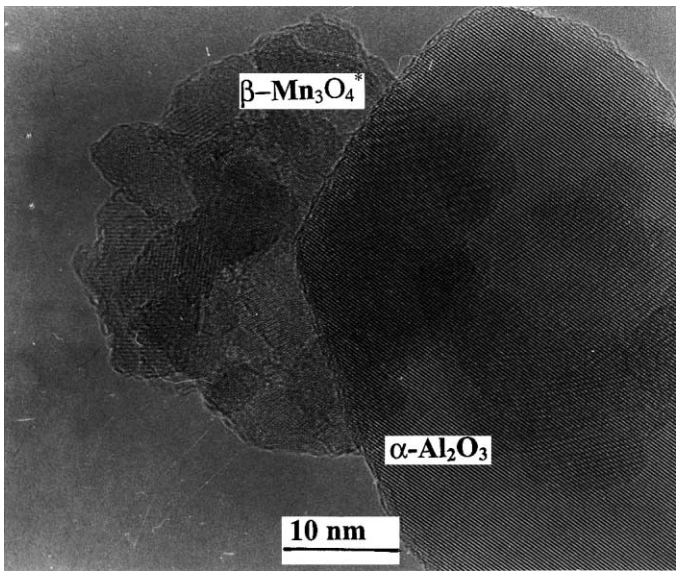

Fig. 3. Micrograph of 10%MnO_x–Al_2O_3 catalyst calcined 3 h at 950 °C.

700^{0}C, 6 hours

1. γ- $Al_2O_3 + Mn^{+2} \longrightarrow [\gamma\text{-}\ Al_2O_3 - Mn^{+3}] + \alpha\text{-}Mn_2O_3$

970^{0}C

2. (1 - 2 h) $\longrightarrow (Mn_{2-x}Al_{1+x}O_{4+\delta}) + [\gamma\text{-}Al_2O_3 - Mn^{+3}] + [\alpha\text{-}Al_2O_3 - Mn^{+3}]$

3. (3 - 4 h) $\longrightarrow$ **[β–Mn_3O_4 - Al^{+3}]** + [δ-Al_2O_3 - Mn^{+3}]+[α - Al_2O_3 - Mn^{+3}]

4. (5 - 6 h) $\longrightarrow$ **[β–Mn_3O_4 - Al^{+3}]** + [δ-Al_2O_3 - Mn^{+3}] + [α -Al_2O_3 - Mn^{+3}]

5. (>10 h) $\longrightarrow$ **[β–Mn_3O_4 - Al^{+3}]** + [α - Al_2O_3 - Mn^{+3}],

Scheme 2.

Based on the XRD and TEM data, the phase transformations that occur in the manganese–alumina as a function of calcination time can be presented in Scheme 2, where $(Mn_{2-x}Al_{1+x}O_{4+\delta})$ and [δ-Al_2O_3–Mn^{3+}] are intermediate phases, [β-Mn_3O_4–Al^{3+}] corresponds to the particles of nanostructured manganese oxide doped with aluminium atoms. The latter was designated in [10] as β-$Mn_3O_4{}^*$.

3.2. XPS results

To obtain data on the surface concentration of different elements in the catalysts, XPS experiments have been carried out. Fig. 4 shows O/Al, Mn/Al and C/Al ratios for samples calcinated at 950 °C for different time. As evident from this figure, the O/Al ratio exhibits a maximum after 2–4 h calcination. The XRD and TEM data suggest that the phase of imperfect cubic spinel of $Mn_{3-x}Al_xO_{4+\delta}$ type forms exactly in this time interval. As it was mentioned above, high concentration of vacancies in this phase indicates that Mn ions are mainly in Mn^{3+} state. When the calcination time increases more than 4 h, Mn ions are reduced partially up to Mn^{2+} state. As a result, there is some oxygen loss in the aluminium–manganese spinel that is evident from the decrease in the O/Al ratio. Gradual character of the Mn reduction was observed also in [9].

It seems likely that a growth of Mn/Al ratio during the first hours of the calcination is associated with diffusion of Mn ions into the structure of alumina support. In addition, the total specific area, initially defined by the γ-alumina support, decreases (see Fig. 5) due to the formation of manganese-modified high-temperature δ- and α-aluminas. Formation of α-Al_2O_3 with a low surface area occurs after calcination of the system for 4 h (see Fig. 5); this process is accompanied by diffusion of Mn ions onto the

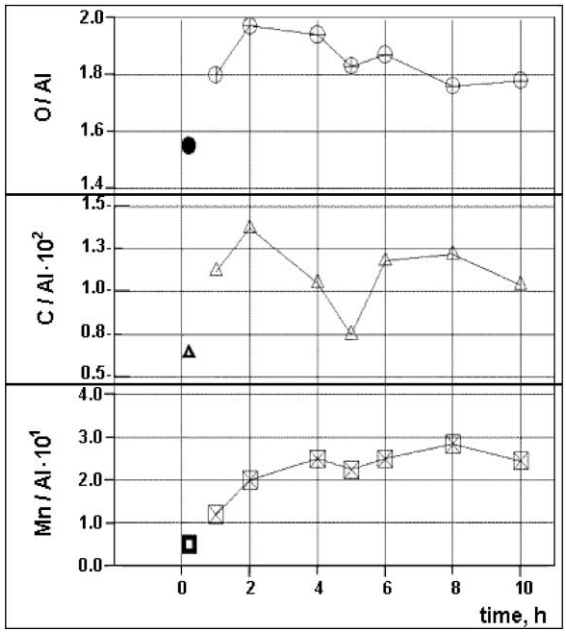

Fig. 4. O/Al, Mn/Al, and C/Al ratios as functions of the calcination time at 950 °C.

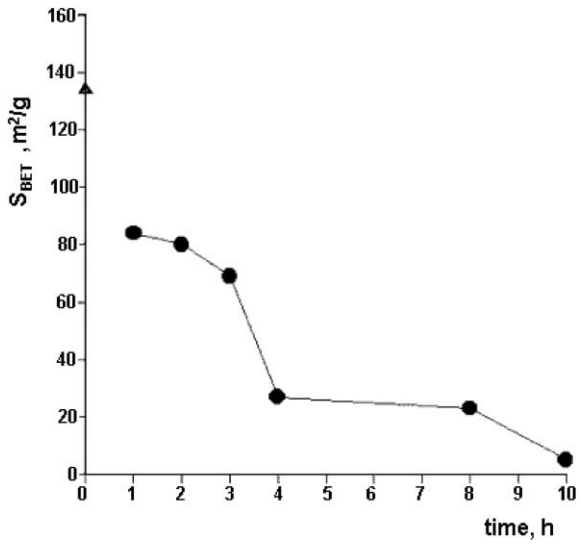

Fig. 5. Dependence BET surface area (in m^2/g) versus time (in h) for 10%MnO_x–Al_2O_3 calcined at 950 °C.

surface of the support particles; these ions have been dissolved previously in the bulk of alumina structure. The latter is a reason for some increase in Mn/Al ratio. Only after 8 h of the calcination, the coalescence of the nanoparticles of manganese-containing phase takes place, and Mn/Al ratio begins to reduce.

The change in C/Al ratio with calcination time is also presented in Fig. 4. Carbon on the catalyst surface (and in the bulk as well) is mainly localized on the defects, therefore, carbon may be considered as a label associated with defects in the catalyst phases. Change of C/Al ratio with time reflects the dynamics of the phase and chemical transformations which occur in the system. Calcination of samples at 950 °C for 2 h causes simultaneous changes in C/Al. The initial increase in C/Al seems to be caused by the formation of the imperfect spinel phase of $Mn_{3-x}Al_xO_{4+\delta}$ type. After calcination of this system for 4 h the imperfect spinel disappears and the C/Al ratio drops off. Further growth of the ratio is likely to be a result of the formation of nanoparticles of manganese-containing phase on the surface of the support after its transformation from γ- to α-Al_2O_3. It should be noted that C/Al ratio changes in the similar way with that of Mn/Al after 5 h calcination of the catalyst.

3.3. Discussion

Thus, XRD, TEM and XPS studies revealed in detail the phase transformation of manganese–alumina catalyst upon calcination at 900–1000 °C. For the first 2 h of the sample calcination, the active diffusion of manganese ions into the structure of γ-alumina and aluminium ions into the bulk of manganese oxide is observed. Active interaction between aluminium and manganese oxides at temperatures above 900 °C may be due to two reasons. Firstly, it is well known that both oxides undergo the structural transformations in this temperature range (α-Mn_2O_3 and γ-Al_2O_3 transform into β-Mn_3O_4 and δ-Al_2O_3, respectively) that strongly increase their reactivity during solid-phase interaction. Second point lies in the fact that structure of β-Mn_3O_4 is similar to that of δ-Al_2O_3 (tetragonal spinel type) that facilitate also the process of the interaction between these two oxides.

Diffusion of Mn ions leads to the formation of metastable solid solutions of manganese ions in the structure of γ- and δ-aluminas; whereas migration of Al ions into the structure of manganese oxide is characterized by the formation of the intermediate phase of $Mn_{3-x}Al_xO_{4+\delta}$ type. Undoubtedly that at the second calcination step ordered manganese–alumina phase of cubic spinel type should be formed due to the release of the oxygen excess from the structure of intermediate phase. However, we observed nanocrystalline aggregates of β-Mn_3O_4 phase modified by Al ions in the sample calcined at 950 °C for 3 h and cooled to the room temperature. To shed the light on this phenomenon we plan to perform further structural study of this system by using in situ high-temperature XRD. We suggest that equilibrium solid solution on the basis of cubic manganese–alumina spinel is formed at the temperature of 900–950 °C. But one can expect that this solid solution is metastable at the room temperature as evident from the phase diagram of quasi-binary aluminium–manganese system [17]. Therefore, metastable solid solution is decomposed after cooling with appearance of small isolated particles of Al-doped β-Mn_3O_4 phase on the surface of α-alumina support. Such nanostructural arrangement of the catalyst seems to be responsible for the optimum catalytic activity in the reaction of *n*-pentane combustion (these data are given in Fig. 6). Coalescence of the active Mn-containing phase upon further calcination (over 6 h) gives rise to the decrease of the catalytic activity of this system.

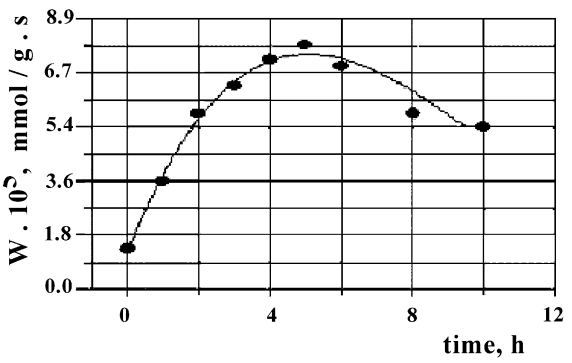

Fig. 6. Activity of 10%MnO_x–Al_2O_3 for the combustion of *n*-pentane in air (300 °C, Co = 0.05 vol.%, X = 50%). The zero abscissa point corresponds to the catalyst calcinated in air at 700 °C for 4 h.

4. Conclusion

The features of phase transformations in the MnO_x/Al_2O_3 system during its calcination at 950 °C for 1–10 h was studied with XRD, TEM and XPS methods. It was found that a set of phase transformations has occurred in the system starting from the unexpected formation (after 1–2 h calcination) of imperfect cubic manganese–alumina spinel with a high concentration of vacancies as well as metastable solid solution of manganese ions in the γ-alumina structure. After further calcination, cubic spinel phase transforms into nanocrystalline aggregates of β-Mn_3O_4 phase modified by aluminium ions, whereas solid solution is decomposed with the formation of α-Al_2O_3 and isolated nanoparticles of β-Mn_3O_4 doped with Al ions and supported on the surface of α-alumina. Such structural arrangement of the active phase is related to the maximum activity exhibited by this catalyst in the reaction of *n*-pentane combustion.

Acknowledgements

The authors thank Prof. A.T. Bell, Berkeley University of California, USA, for fruitful and friendly discussion. This work was supported by Russian Foundation for Basic Research, Grant No. 99-03-32135a.

References

[1] L.L. Gogin, Yu.Sh. Matros, A.G. Ivanov, Ecology and Catalysis, Nauka, Novosibirsk, 1990, p. 107.
[2] Yu.Sh. Matros, G.A. Bunimovich, Catal. Rev.-Sci. Eng. 38 (1996) 1.
[3] P.G. Tsyrulnikov, S.A. Stuken, E.N. Kudrja, V.A. Balashov, O.A. Kachkina, V.A. Lyubushkin, O.V. Atamanchuk, US Patent 5 880 059 (1999).
[4] M.F.M. Zwinkels, S.G. Jaras, P.G. Menon, T.A. Griffin, Catal. Rev.-Sci. Eng. 35 (1993) 319.
[5] L.D. Pfefferle, W.C. Pfefferle, Catal. Rev.-Sci. Eng. 29 (1987) 219.
[6] Z.R. Ismagilov, M.A. Kerzhentsev, Catal. Rev.-Sci. Eng. 32 (1990) 51.
[7] P.G. Tsyrulnikov, V.S. Salnikov, V.A. Drozdov, S.A. Stuken, A.V. Bubnov, E.I. Grigorov, A.V. Kalinkin, V.I. Zaikovskii, Kinet. Katal. 32 (1991) 439.
[8] P.G. Tsyrulnikov, Catalysis and Catalysts, Fundamental Investigations of Institute of Catalysis, Boreskov Institute of Catalysis, Novosibirsk, 1998, p. 39.
[9] D.I. Kochubeii, V.V. Kriventsov, G.N. Kustova, G.V. Odegova, P.G. Tsyrulnikov, E.N. Kudrja, Kinet. Katal. 39 (1998) 294.
[10] S.V. Tsybulya, G.N. Kryukova, A.A. Vlasov, N.N. Boldyreva, O.N. Kovalenko, P.G. Tsyrulnikov, React. Kinet. Catal. Lett. 64 (1998) 113.
[11] D. Briggs, M.P. Seach, Practical Surface Analysis by Auger and X-ray Photoelectron Spectroscopy, Wiley, Chichester, 1983.
[12] E.M. Moroz, V.N. Kuklina, V.A. Ushakov, Kinet. Katal. 28 (1987) 699.
[13] S.V. Tsybulya, L.P. Solovyeva, G.N. Kryukova, E.M. Moroz, Zurn. Strukt. Chim. 32 (1991) 18.
[14] G.N. Kryukova, D.O. Klenov, A.S. Ivanova, S.V. Tsybulya, J. Eur. Ceram. Soc. 20 (2000) 1187.
[15] JCPDS Powder Diffraction File No. 29-8803.
[16] P.G. Tsyrulnikov, O.N. Kovalenko, L.L. Gogin, T.G. Starostina, A.S. Noskov, A.V. Kalinkin, G.N. Kryukova, S.V. Tsybulya, E.N. Kudrja, A.V. Bubnov, Appl. Catal. A 167 (1998) 31.
[17] E.H.L.J. Dekker, G.D. Rieck, Z. Anorg. Allg. Chem. B 415 (1975) 68.